(23) M. Bixon and J. Jortner, *J. Chem. Phys.*, **48**, 715 (1968); J. Jortner, S. A. Rice, and R. M. Hochstrasser, *Adv. Photochem.*, **7**, 149 (1969).
(24) N. Mataga and O. Tanimoto, *Theor. Chim. Acta*, **15**, 111 (1969).
(25) J. Jortner and G. C. Morris, *J. Chem. Phys.*, **51**, 3689 (1969).
(26) It was pointed out from quite a general viewpoint that the interaction of the charge-transfer and donor-excited states was much larger than that of the charge-transfer and acceptor-excited states for contact donor–acceptor pairs: J. N. Murrell, *J. Am. Chem. Soc.*, **81**, 5037 (1959).

Molecular Orbital Studies of Electron Donor–Acceptor Complexes. 3. Energy and Charge Decomposition Analyses for Several Strong Complexes: $OC-BH_3$, H_3N-BH_3, $CH_3H_2N-BH_3$, $(CH_3)_3N-BH_3$, and H_3N-BF_3

Hideaki Umeyama and Keiji Morokuma*

Contribution from the Department of Chemistry, University of Rochester, Rochester, New York 14627. *Received January 15, 1976*

Abstract: The interaction energies of five strong EDA complexes were analyzed in terms of electrostatic, exchange, polarization, and charge transfer components as functions of intermolecular separation and orientation. Decompositions of intermolecular forces and charge distributions were also performed. The $OC-BH_3$ complex is found to be a strong complex because of large charge-transfer and electrostatic energies. A deviation from the most favored C_{3v} approach results in a decrease in electrostatic stabilization, approach of the O end of CO to BH_3 is less desirable due to a decrease in charge-transfer energy, and the planar BH_3 forms a less stable complex than the pyramidal BH_3 as a result of increased exchange repulsion. The principal contribution to H_3N-BH_3 stabilization is the electrostatic interaction. The H_3N-BH_3 rotational barrier is due to exchange repulsion, while the small methyl substituent effect is due to a cancellation of the effects of polarization and exchange interactions.

I. Introduction

Numerous studies have been published on "electron donor–acceptor (EDA) complexes" concerning their structures, bonding characteristics, and spectroscopic, electric, and other physical properties.[1] A particularly interesting and difficult theoretical question concerns the origin of stabilization, i.e., the relative importance of electrostatic and charge transfer forces in the ground state of the complex. As is evident from Mulliken's characterization of these complexes as "charge-transfer complexes", earlier work was predicated on the belief that the stabilization was principally due to the charge transfer force.[2] Later Hanna et al.[3] argued that in benzene–halogen complexes the electrostatic interaction, in particular the quadrupole-induced dipole interaction, is the principal binding force. Mulliken and Person have proposed that the electrostatic forces are likely to dominate the binding only in weak EDA complexes.[4] Quantum chemical calculations should be able to provide insight for this important problem.

The energy and charge distribution decomposition analyses have been successfully used for the elucidation of the origin of hydrogen bonding in ground and excited states.[5-11] The method of Morokuma and co-workers[5-9] decomposes the interaction energy ΔE, utilizing clear definitions within the molecular orbital framework, into energy components—electrostatic (E_{ES}), exchange repulsion (E_{EX}), polarization (E_{PL}), charge transfer (E_{CT}), and the coupling term (E_{MIX}).

These interactions may be conceptually viewed in the following manner. ES is the classical interaction between the undistorted charge distributions on the monomers A and B, including dipole–dipole and all higher order terms. PL is the energy change resulting from the distortion of electron clouds of one monomer by the presence of the other and vice versa. EX is a direct consequence of the Pauli principle which dictates that electrons on the two molecules not occupy the same portion in space. CT is the interaction of occupied MO's of A with vacant MO's of B and vice versa and causes electron delocalization and charge transfer. MIX is the sum of various coupling terms between the above-mentioned components and is delivered as a difference between the total interaction energy ΔE and the sum of the above four terms.

It has been found that near the equilibrium geometry of most hydrogen bonded complexes the electrostatic and charge transfer (both attractive) energies and the exchange repulsion are the three major contributors of nearly comparable magnitude, one part of the attraction cancelling with the repulsion. It has also been recognized that the electrostatic interaction alone is often sufficient to predict the relative direction with which the proton donor and the acceptor approach each other.

Considering the fact that numerous ab initio studies have been carried out for hydrogen-bonded complexes,[5-9,12-13] it is surprising that only a handful of ab initio calculations have been published for EDA complexes.[9,14-22] The energy decomposition analysis has recently been applied to several weak $n-\pi$ and $\pi-\pi$ type EDA complexes, including $(CN)_2CO\cdots H_2O$, $(CN)_2C{=}C(CN)_2\cdots H_2O$, $H_2CO\cdots C_2H_4$, and $(CN)_2CO\cdots C_6H_6$. For the first two complexes, the electrostatic energy was found to be by far the most important contributor near the equilibrium geometries.[15] In the latter two, which are very weak complexes, the electrostatic, charge transfer, exchange repulsion, and dispersion energies are all of approximately equal importance.[16]

In order to gain additional insight into the nature and origin of bonding in EDA complexes, we have performed energy and charge distribution analyses for the ground state of the "strong" complexes, $OC\cdots BH_3$, $H_3N\cdots BH_3$, $(CH_3)H_2N\cdots BH_3$, $(CH_3)_3N\cdots BH_3$, and $H_3N\cdots BF_3$. Previous calculations for some of these systems include: Fujimoto, Kato, et al. ($OC-BH_3$ and H_3N-BH_3),[18] Armstrong, Perkins, et al. ($OC-BH_3$, H_3N-BH_3, and H_3N-BF_3),[20] Veillard (H_3N-BH_3),[21] and

Palke (H_3N-BH_3).[22] In the present paper we present a detailed analysis for each of the individual complexes as well as comparisons between similar complexes. In section II we present briefly computational methods and geometries. Section III focuses on the results for OC-BH_3 including energy, force and electron density decomposition, the effect of back donation, angular dependency, and various modes of approaches. In section IV we present results for borazane and its derivatives and include comparisons with the OC-BH_3 complex and the protonated complexes of amines. Section V is a short general discussion.

II. Computational Methods and Monomer Geometries

All calculations were performed within the framework of closed-shell single-determinant ab initio LCAO SCF-MO theory, using the GAUSSIAN 70 programming system.[23] The split-valence 4-31G basis set was used with the suggested standard scale factors.[24] This set is flexible enough to give a reasonable estimate of interaction energies; however, it does have a tendency to overestimate the polarity of the isolated molecules. This is reflected in exaggerated dipole moments and, consequently, overestimates in the electrostatic interaction.[6,9]

Monomer Geometries. In all calculations it was assumed that the geometries of isolated electron donors, CO, NH_3, NH_2-CH_3, and $N(CH_3)_3$, were not altered upon complex formation. Taken from experiments are: for CO, r(CO) = 1.13 Å;[25] for NH_3(C_{3v}), r(NH) = 1.0124 Å and ∠HNH = 106.67°;[26] and for $N(CH_3)_3$ (C_{3v}), r(CN) = 1.451 Å, r(CH_s) = 1.109 Å, r(CH_a) = 1.088 Å, ∠CNC = 110.9°, ∠NCH_s = 111.7°, ∠NCH_a = 110.1°, ∠H_aCH_s = 108.1°, and ∠H_aCH_a = 108.6°,[27] where the H_s is on a symmetry plane and two H_a's are not. Methylamine was assumed to have the same geometry as trimethylamine, except that r(NH) = 1.0124 Å. For BH_3 and BF_3 two geometries were studied, a planar (D_{3h}) configuration, which is the most stable monomer configuration, and a pyramidal (C_{3v}) configuration, which is the expected conformation in the complexed forms.[26] The geometries used were: for BH_3(D_{3h}), r(BH) = 1.19 Å;[22,28] for BH_3 (C_{3v}), r(BH) = 1.19 Å and ∠HBZ = 106.3° (Z is the C_{3v} axis); for BF_3 (D_{3h}), r(BF) = 1.30 Å; for BF_3 (C_{3v}), r(BF) = 1.38 Å and ∠FBZ = 107.9 Å. All these are based on theoretical studies except for the last two, which were taken from experimental results for F_3B-NH_3.

Energy Decomposition Analysis. The energy decomposition analysis was performed with the method of Morokuma[5] and Kitaura and Morokuma.[8] The electron distribution was separated into components using the method of Yamabe and Morokuma.[7] The formal aspects of these schemes have been described elsewhere; however, the practical procedures which we followed are summarized in the Appendix, in part to answer several inquiries. The decomposition of the energy into E_{ES}, E_{PL}, E_{EX}, and $E_{CT} + E_{MIX}$ necessitates only two SCF calculations using a standard SCF program. The decomposition of E_{CT} and E_{MIX} requires a special SCF program based on MO's rather than AO's. The analysis described above is applicable only if one assumes that the monomer geometries do not change upon formation of a complex. If the effects of intramolecular geometry changes are explicitly considered, the method proposed by Umeyama, Kitaura, and Morokuma is required.[29] Within the Hartree-Fock framework the dispersion energy cannot be taken into account. In the strong EDA complexes being studied in this paper the dispersion energy is not expected to be a significant contribution to the total interaction. Individual energy components are more sensitive to the choice of basis functions and geometry optimization than the total interaction energy. Nonetheless, our past experience shows that general qualitative features of a decomposition are not strongly dependent on the basis set.[6,9]

A word of warning is in order against overinterpreting the energy decomposition results presented in this paper. Energy components are more sensitive to geometry optimization and the basis functions than is the total interaction energy. Components depend particularly strongly on the intermolecular separations, so that care has to be taken when two different relative orientations or complexes are compared. Since the 4-31G basis set overestimates the polarity of component molecules, the contribution of ES tends to be overemphasized. Previous experiences[5-11] suggest that qualitative conclusions derived from the analysis are rather insensitive to the basis set used. When the intermolecular separation is small and the interaction is strong, the coupling term E_{MIX} can become as large as the absolute values of the other individual components. E_{MIX} is calculated as the residue left behind when the sum of components ($E_{ES} + E_{PL} + E_{EX} + E_{CT}$) is subtracted from the total interaction energy ΔE. Since PL and CT terms are each calculated in the absence of all other interactions except ES, the included term tends to "overreact" in order to attain maximum stabilization. The large and positive E_{MIX} reflects the fact that the EX-CT, EX-PL, and CT-PL coupling terms must compensate for the overestimate of PL and CT. One may argue that when the coupling term is as large as the absolute values of the other components, some significance of the analysis is lost. The interaction is too strong to decompose meaningfully into components. We feel that each individual component is still as meaningful as its definition implies: it is the interaction in the absence of all other components except ES. One should not, however, fail to take into account the contribution of MIX when one analyzes a strong interaction, because it may change qualitative characteristics of the decomposition.

Calculation of Force Components. In the analysis of the bonding of complexes, it is convenient to calculate derivatives of energy components along the approach path of interacting molecules. The derivatives are obtained by fitting an energy component to a continued fraction, which is then differentiated analytically.[30] A continued fraction is given by

$$C_N(R) = \left(\frac{E(R_1)}{1+}\right)\left(\frac{a_1(R-R_1)}{1+}\right)\left(\frac{a_2(R-R_2)}{1+}\right) \cdots \left(\frac{a_N(R-R_N)}{1}\right)$$

where a_l is evaluated recursively:

$$a_l = \frac{1}{R_l - R_{l+1}}\left\{1 + \left(\frac{a_{l-1}(R_{l+1}-R_{l-1})}{1+}\right) \times \left(\frac{a_{l-2}(R_{l+1}-R_{l-2})}{1+}\right) \cdots \left(\frac{a_1(R_{l+1}-R_1)}{1-[E(R_1)/E(R_{l+1})]}\right)\right.$$

with

$$a_1 = \{[E(R_1)/E(R_2)] - 1\}/(R_2 - R_1)$$

The continued fraction goes through each of the input points $\{E(R_l), l = 1, 2, \cdots, N+1\}$ and is numerically stable for a wide range of R. The derivative of the continued fraction may be evaluated analytically:

$$\frac{dC_N(R)}{dR} = \frac{-E(R_1)}{(1+Z_1)^2}\frac{1}{1+Z_2} \times \left\{a_1 - \frac{Z_1}{1+Z_3}\left[a_2 - \frac{Z_2}{1+Z_4} \times \left(\cdots\left\{a_{N-1} - \frac{Z_{N-1}}{1}a_N\right\}\cdots\right)\right]\right\}$$

where

$$Z_l = \left(\frac{a_l(R-R_l)}{1+}\right)\left(\frac{a_{l+1}(R-R_{l+1})}{1+}\right)\cdots a_N(R-R_N)$$

Table I. Energy Decomposition Analysis for the Complex OC-BH_3 as a Function of $R = r$(C···B), C_{3v} Approach[b]

R, Å	1.37	1.57	1.63[a]	1.77	2.00	2.30	2.50	2.70	3.00
ΔE	−15.7	−27.9	−28.5	−24.5	−17.8	−11.3	−8.4	−6.3	−4.1
ES	−110.5	−70.0	−60.9	−42.2	−23.0	−10.4	−6.3	−4.0	−2.2
EX	217.0	118.8	98.9	63.3	30.0	10.6	5.2	2.5	0.8
PL	−196.4	−82.2	−61.8	−33.0	−11.5	−3.1	−1.4	−0.7	−0.3
CT	−211.5	−89.5	−68.3	−40.3	−19.7	−9.5	−6.3	−4.3	−2.5
MIX	285.8	95.0	63.6	27.4	6.3	1.2	0.5	0.2	0.1

[a] Equilibrium values obtained from a parabolic fit of calculations at 1.37, 1.57, and 1.77 Å. [b] Values given are in kilocalories per mole.

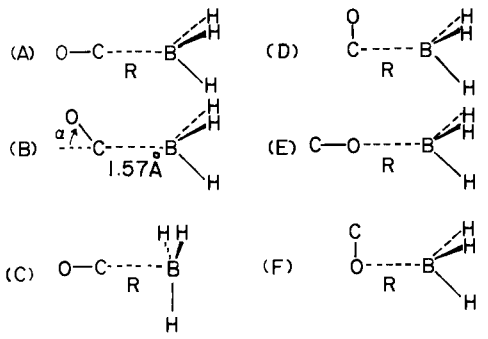

Figure 1. Various modes of approaches between OC and BH_3.

III. Borane Carbonyl (OC-BH_3)

A. Energy Decomposition Analysis. First, we examined the interaction energy components as functions of the intermolecular separation $R = r$(C···B) as the B end of pyramidal BH_3 (prepared in advance) approaches the C end of C=O, maintaining the overall C_{3v} symmetry (Figure 1A). The results are shown in Table I. The interpolated equilibrium separation R = 1.63 Å is in good agreement with the experimental value of 1.57 Å.[25] The stabilization energy, ΔE = −28.5 kcal/mol, at the minimum relative to CO and pyramidal BH_3 plus the energy, 17.0 kcal/mol, required to form a pyramidal BH_3 from a planar BH_3 yield a net energy of reaction of −11.5 kcal/mol for the formation of the complex. An experimental value is $\Delta H°_{300}$ = −18.8 kcal/mol.[31] In order to compare the theoretical result with the experimental value more quantitatively, one must include the zero point energy difference and the correlation corrections.[20] We will not carry this out, because the comparison per se is not the goal of the present paper.

At the equilibrium separation all three attractive components, ES, PL, and CT, are large and of a comparable magnitude. They are all essential for stabilization of this complex. At this, as well as at smaller separations, the coupling term E_{MIX} is found to be positive and as large as each attraction term. This result may be explained in the following manner. The polarization and charge transfer terms are each calculated in the absence of all other interactions except electrostatic (see Appendix). Consequently, when R is small and the interaction is strong, the included term tends to "overreact" in order to attain maximum stabilization. The positive nature of E_{MIX} reflects the fact that the EX-CT, EX-PL, and CT-PL couplings must compensate for the overestimate of PL and CT. At a larger intermolecular separation 2.7–3.0 Å, where weak complexes typically have their maximum stabilization, the importance of various interactions is quite different. The two principal contributors there are ES and CT. The large CT stabilization at the 2.7–3.0 Å range is rather unique to this strong complex. Weak complexes typically have a negligible CT at such a distance.[15,16]

As a vehicle for demonstrating the critical importance of each attractive component, we plotted as a function of R the interaction energy ΔE^{tr} in which one attractive component (ES, PL, or CT) was omitted. The equilibrium R_e^{tr} and the corresponding truncated interaction energy ΔE_e^{tr} for each truncation are given in Table II as well as the untruncated equilibrium distance and interaction energy. It is evident from the table that the complex without PL is also rather weak. Though the truncation does not take MIX into account, its effect on R_e^{tr} is expected to be small because MIX is not important near R_e^{tr}. We may conclude, therefore, that all three attractive components are essential for formation of this strong complex.

Table II. Truncated Interaction Energy ΔE^{tr} and Equilibrium Separation R_e^{tr} for OC-BH_3, C_{3v} Approach

ΔE^{tr}	R_e^{tr}, Å	ΔE_e^{tr}, kcal/mol
ΔE	1.63	−28.5
ΔE-E_{ES}	2.71	−2.3
ΔE-E_{PL}	2.28	−8.2
ΔE-E_{CT}	2.55	−2.2

B. Force Decomposition Analysis. The energy decomposition analysis enables one to determine the contribution of individual energy components to the total interaction energy for a given geometry. It does not allow, however, a determination of which components are responsible for the attractive force which causes the intermolecular separation, R, to decrease and the interaction energy to become more negative. This requires the calculation of the components of energy gradient in the direction of intermolecular approach. As was described in the previous section, this was accomplished by analytical differentiation of a continued fraction fit to the interaction potential. The components of the total force are shown in Figure 2. At the equilibrium separation ($R_e \sim 1.63$ Å) the total force ($F = -d\Delta E/dR$) must be zero. Consequently, the repulsive force is balanced by the attractive force: $-dE_{EX}/dR - dE_{MIX}dR = -dE_{ES}/dR - dE_{PL}/dR - dE_{CT}/dR$. Near R_e the relative importance of the attractive forces are dES ~ 20% (d denotes a force), dPL ~ 40%, and dCT ~ 40%; the two short-range components being more important than the long range dES. At a larger separation ($R \sim 2.70$ Å), the relative contributions are dES ~ 46%, dPL ~ 12%, and dCT ~ 42%. As was noted in section IIIA, the significance of dCT even at this large separation is an indication of the uniquely important role of CT in this strong complex.

C. Electron Density Decomposition and Population Analyses. As an aid for analysis, the changes of components of σ and π atomic gross population at R = 2.70 and 1.57 Å are shown in Table III. The CT and PL density maps at R = 2.70 Å are shown in Figure 3 and all the component density maps at R = 1.57 Å are presented in Figure 4.

As is seen in Table III, at a separation of 2.70 Å, a charge transfer of 0.06 e takes place from CO to BH_3, predominantly from the C atom to the B atom. This is also clearly demonstrated in the CT density map of Figure 3. The population analysis indicates that no significant transfer of π electrons occurs at this separation. A large polarization occurs within

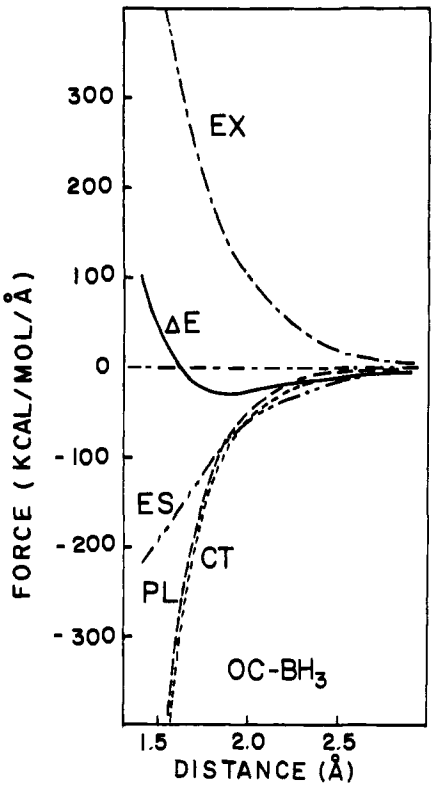

Figure 2. Force components along the separation R for the complex OC-BH_3 in the C_{3v} approach as functions of $R = r(C\cdots B)$.

Table III. Change of Components of Gross Atomic Population in the Complex OC-BH_3, C_{3v} Approach[a]

	EX	PL	CT + MIX	Total
		R = 2.70 Å		
Oσ	−0.000	0.018	0.010	0.028
π	0.000	−0.010	−0.003	−0.013
Cσ	0.000	−0.018	−0.068	−0.086
π	−0.000	0.010	0.005	0.015
Bσ	−0.002	−0.013	0.056	0.041
π	−0.000	−0.011	−0.001	−0.011
Hσ	0.001	0.004	−0.001	0.006
π	0.000	0.004	−0.000	0.003
$BH_3\sigma^b$	0.0	0.0	0.058	0.058
π	0.0	0.0	−0.002	−0.002
		R = 1.57 Å		
Oσ	−0.004	0.138	−0.089	0.045
π	0.007	−0.011	−0.012	−0.016
Cσ	0.004	−0.138	−0.227	−0.361
π	−0.007	0.011	0.107	0.111
Bσ	−0.048	0.419	−0.144	0.227
π	−0.002	−0.035	0.021	−0.016
Hσ	0.016	−0.140	0.153	0.030
π	0.001	0.012	−0.038	−0.026
$BH_3\sigma'^b$	0.0	0.0	0.316	0.316
π	0.0	0.0	−0.095	−0.095

[a] Positive and negative values indicate an increase and a decrease, respectively, of electron population upon complex formation. [b] The sum for all the atoms of BH_3. The sums for CO are negatives of the BH_3 values.

CO, resulting in the polarization along the bonds $-\delta+\delta C^{-\delta}-{}^{+\delta}O-\delta+\delta$, as was typically observed in many hydrogen-bonded and protonated complexes.[7,10] This is accompanied by a smaller polarization of BH_3. At the separation 1.57 Å, corresponding to a near equilibrium geometry, as is expected from the large interaction energy terms of Table I, large changes of

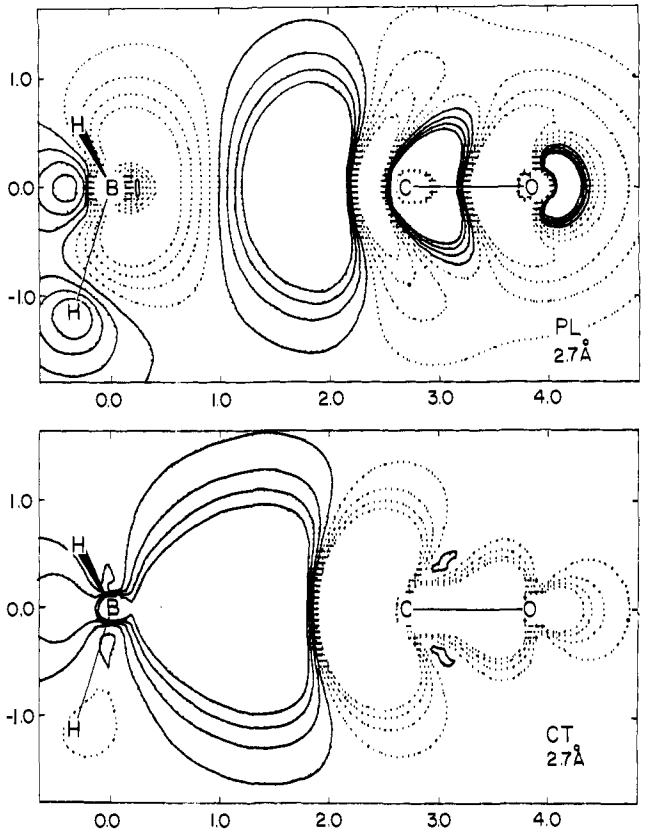

Figure 3. Component electron density maps for the complex OC-BH_3 at $r(C\cdots B)$ = 2.70 Å in the C_{3v} approach. Full lines indicate density increases and dotted lines indicate decreases. Contours indicated are, successively, $\pm1, \pm3, \pm5, \pm7 \times 10^{-4}$ (Bohr^{-3}). The coordinates are in angstroms relative to the boron atom and the plotting is made for an HBCO plane.

component atomic population take place. An extensive polarization of BH_3 and CO and a large charge transfer can be observed in Table III and Figure 4. The CT density map (Figure 4) at this separation is very different qualitatively from that at 2.70 Å (Figure 3). Here the electron density has accumulated in the entire B···C intermolecular region, suggesting formation of a strong σ bond. It is interesting to note that in almost all the cases in Table III the π-atom population changes have an opposite sign to the corresponding σ-atom population changes. This is probably, as will be discussed later, due to the dual characteristics of CO, having a $C^- {}^+O$ polarity for σ electrons and a $C^+ {}^-O$ polarity for π electrons. The population analysis suggests that at this separation 0.32 e of σ charge is transferred from CO to BH_3 and 0.10 e × 2 of π charge is back-donated from the BH_3 to CO. The donation and back-donation will be analyzed more in the next section.

D. Charge Transfer and Back-Donation. In analyzing energy components of molecular interactions, it is sometimes informative to further separate the charge transfer energy into the contribution of CT from A to B and that from B to A. This type of analysis should be particularly appropriate here due to the apparent complexity of the charge transfer interaction in H_3B-CO. The energy decomposition scheme of Kitaura and Morokuma can handle this situation.[8] By including only the block connecting the occupied MO's of A and the vacant MO's of B as well as the diagonal block in the Hartree-Fock matrix, one can obtain $CT_{A\to B}$. The $B_{occ} \to A_{vac}$ and diagonal blocks gives $CT_{B\to A}$. The inclusion of both $A_{occ} \to B_{vac}$ and $B_{occ} \to A_{vac}$ blocks as well as the diagonal block leads to the total CT which has been used in the previous sections. The difference between CT and $CT_{A\to B} + CT_{B\to A}$ should be called a coupling term CT_{MIX} between the two CT directions. Therefore, $E_{CT} = E_{CT_{A\to B}} + E_{CT_{B\to A}} + E_{CT_{MIX}}$. Similarly, the CT component

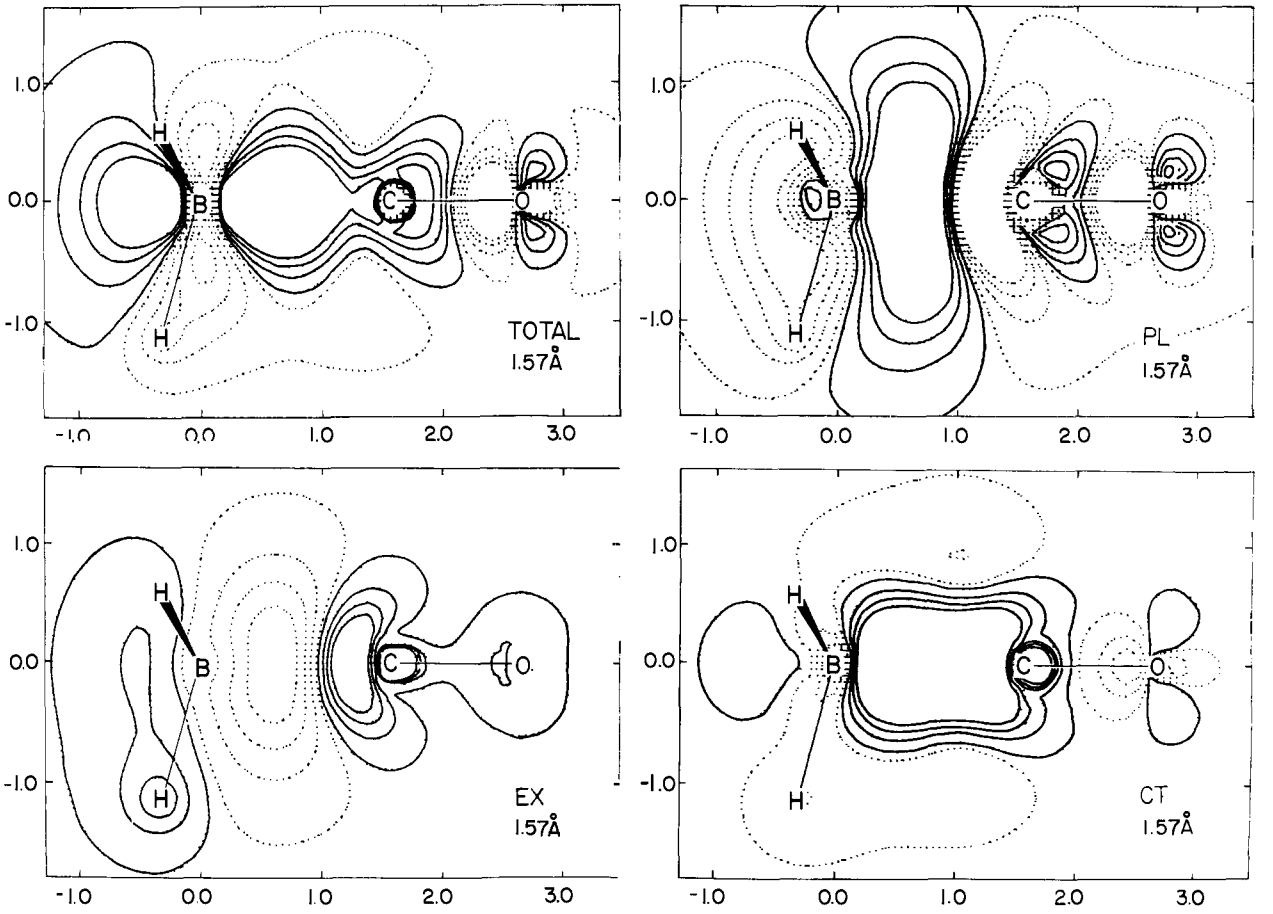

Figure 4. Component electron density maps for the complex OC-BH_3 at r(C···B) = 1.57 Å in the C_{3v} approach. Contours indicated are, successively, ±1, ±5, ±9, ±13 × 10^{-3} (Bohr^{-3}). For other details, see Figure 3.

Table IV. Further Decomposition of Charge Transfer Energy in the C_{3v} Complex OC-BH_3 at Various Separation $R = r$(C···B)[a]

	R, Å 1.77	2.00	2.30	2.70
CT	−40.3	−19.7	−9.5	−4.3
$CT_{OC\leftarrow BH_3}$	−12.7	−4.9	−1.5	−0.4
$CT_{OC\rightarrow BH_3}$	−26.5	−14.2	−7.8	−3.9
CT_{MIX}	−1.1	−0.5	−0.2	−0.0

[a] Values given in kilocalories per mole.

of the electron density may be further divided into three terms

$$\rho_{CT} = \rho_{CT_{A\rightarrow B}} + \rho_{CT_{B\rightarrow A}} + \rho_{CT_{MIX}}$$

Such an analysis of the charge transfer interaction has been performed for the OC-BH_3 complex in the C_{3v} approach at various intermolecular separations $R = r$(C···B). As is seen in Table IV, at a large separation the CT energy is predominantly due to charge transfer from CO to BH_3. Near the equilibrium separation, the OC → BH_3 forward charge transfer is still the most important term, although the back donation from BH_3 to CO does make a significant contribution. An estimate of the relative importance at equilibrium ($R \sim 1.63$ Å) is OC → BH_3/OC ← $BH_3 \sim 2/1$. Though this magnitude will depend sensitively on the basis set, this probably is the first semiquantitative demonstration of the importance of back-donation from the strongly hyperconjugating π orbital of BH_3 to the low lying π^* orbital of the carbonyl group.

The two CT components of the electron density map are shown in Figure 5. The charge transfer from CO to BH_3 is found to be predominantly within the σ framework, while the back charge transfer from BH_3 to CO is principally within the π framework. This is reflected in the changes of σ and π populations in Table III.

E. Angular Dependency near the Equilibrium Separation. For better understanding of the origin of interactions in molecular complexes, it is extremely useful to establish for the OC-BH_3 complex that the C_{3v} geometry is the most stable one and why that is the case. In order to study this problem we examined conformations in which the C-O axis was skewed from the C_{3v} axis by an angle α. These rotations were such that the C atom remained on the C_{3v} axis of the BH_3 moiety with $R = r$(C···B) = 1.57 Å and such that OC-BH were in a staggered configuration. This is illustrated in Figure 1B. Results of stabilization energy and energy decomposition relative to the C_{3v} approach ($\alpha = 0$) are shown in Table V. The C_{3v} geometry is found to be the most stable, in agreement with experiments,[26] and the energy increases quadratically with α. It is clear from Table V that the stability of the C_{3v} approach is primarily due to a more favorable electrostatic interaction and, to a lesser extent, to the charge transfer interaction. The loss of ES with α can be understood in terms of the peculiar electron distribution of CO. In the ground state of CO,[32] whose electron configuration is $\sigma^{10}\pi^4$, triple bonding π electrons are polarized toward the oxygen atom (with the 4-31 set, the π-electron population for each of x and y direction on C is 0.47). The six valence σ electrons, on the other hand, form a C-O σ bond, an O lone pair, and a C lone pair, leaving a substantial negative net σ charge on C (with the 4-31 set, the net σ charge on C is $-\delta = -0.66$ and that on O is $+\delta$). The charge distribution of CO, therefore, may be schematically represented as: $-\delta C^{+\delta'}-{}^{-\delta'}O+\delta$. The electrostatic interaction is most favored when the electron deficient B end of BH_3 approaches the C end of CO

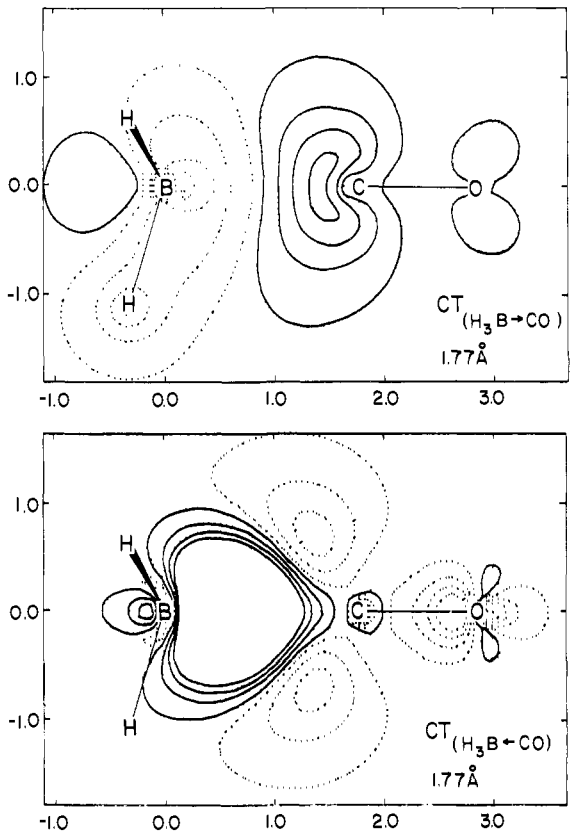

Figure 5. Density maps of forward and back charge transfer components for the complex OC-BH_3 at r(C···B) = 1.77 Å in the C_{3v} approach. Contours indicated are, successively, ±0.5, ±2.0, ±3.5, ±5.0 × 10^{-3} (Bohr^{-3}). For other details, see Figure 3.

along the extension of the OC axis. As α increases, the B atom approaches more closely toward the positive π side of CO, resulting in a decrease in the electrostatic stabilization. The reduction of the charge transfer interaction upon a deviation from C_{3v} orientation may be attributed mainly to the decrease of overlap between the highest occupied 5σ MO of the electron donor CO and the lowest vacant $3a_1$ (σ) MO of BH_3. Table V indicates that as α increases the exchange repulsion at first decreases and then increases after $\alpha \sim 60°$. The initial decrease may be interpreted as resulting from a decrease in the overlap between σ-electron clouds of CO and BH_3. Its eventual increase is probably due to the overlap of electron clouds of the oxygen atom with those of the BH bonds.

F. Planar BH_3 Approaching CO. The BH_3 molecule is predicted to be planar in the isolated molecule, whereas it is pyramidal in the complex. A method has been proposed to carry out energy decomposition along the reaction coordinate on which constituent molecules change geometries as they approach each other.[29] It is rather tedious, however, to find the reaction coordinate in a multidimensional space. Instead, a series of calculations was carried out for an approach of planar BH_3 to the C end of CO maintaining the overall C_{3v} symmetry (Figure 1C). The results of the calculations are shown in Table VI with the reference isolated monomers being CO and BH_3 (D_{3h}). This case may be considered an extreme reaction path, where rigid reactant molecules first form a complex and then relax their geometries, whereas calculations in Table I are the other extreme, where reactants first change themselves to the anticipated complex geometries and then form a complex. The reference of energy decomposition in Table I was CO + BH_3 (C_{3v}). It is evident from Tables I and IV that the greater molecular interaction for pyramidal BH_3 at large separations (2.7-2.3 Å) is the result of a decrease in the exchange repulsion. All other interaction components are nearly independent of what form of BH_3 is considered. Though the situation is not very clear at a shorter distance (1.57 Å), the exchange repulsion still appears to be the principal difference between Tables I and VI. We may conclude that BH_3 prefers the pyramidal structure in the complex in order to reduce the exchange repulsion.

Table V. Relative Energy Decomposition Analysis for the Complex OC-BH_3 at Various Rotations (α) of the Oxygen Atom from the C_{3v} Axis at the Separation 1.57 Å[a]

	α 30°	60°	90°
$\Delta\Delta E$	10.2	41.6	91.5
ΔES	12.8	42.7	59.6
ΔEX	−3.5	−8.5	18.2
Δ(PL + MIX)	−8.8	−20.9	−19.7
ΔCT	9.6	28.3	33.5

[a] Energies are in kilocalories per mole relative to the C_{3v} (α = 0) values.

Table VI. Energy Decomposition Analysis for the Complex OC-BH_3, where BH_3 Remains Planar at Various Separations R = r(C···B),[a] C_{3v} Approach

R, Å	1.57	2.30	2.70
ΔE	5.3	−2.8	−3.0
ES	−88.4	−10.8	−3.5
EX	180.5	17.8	4.3
PL	−112.3	−2.3	−0.4
CT	−146.9	−8.6	−3.4
MIX	172.4	1.2	0.0

[a] Values given in kilocalories per mole.

Table VII. Energy Decomposition Analysis for the Complex OC-BH_3 for the Approach of Figure 1D, where CO Is Perpendicular to the C_{3v} Axis and C Is on the C_{3v} Axis, at Various Separations R = r(C···B)[a]

R, Å	1.57	1.90	2.30	2.70	3.10
ΔE	63.6	23.4	7.2	2.3	0.9
ES	−10.4	−0.4	3.0	2.6	1.7
EX	137.0	46.7	11.4	2.6	0.5
PL + MIX	−6.9	−4.2	−0.6	−0.1	−0.1
CT	−56.0	−18.7	−6.6	−2.7	−1.2

[a] Values given in kilocalories per mole.

G. Various Modes of Approaches. In most of the previous sections we assumed a mode of approach in which CO approaches from the C end collinearly to the B atom of BH_3. In order to examine whether this is the most favored approach and, if so, why, we now examine three other modes of approaches, as illustrated in Figures 1D-F.

Table VII shows the results for the approach of Figure 1D, where the CO is perpendicular to the C_{3v} axis of BH_3 and C is on the C_{3v} axis with an OC-BH in a staggered conformation. This geometry, near the equilibrium separation, was also included in section IIIE. A comparison of the results in Tables VII and I reveals that the perpendicular approach is less favored than the collinear approach. The instability is principally due to the lack of electrostatic attraction, supplemented in part for smaller separations by a decrease in the charge transfer stabilization. As was discussed in section IIIE, the electrostatic repulsion is caused by interaction of the electron-deficient π side of the carbon atom and the electron-deficient end of BH_3.

Table VIII. Energy Decomposition Analysis for the Complex CO-BH_3, where CO Is on the C_{3v} Axis and O Is Approaching BH_3, at Various Separations $R = r(O\cdots B)$[c]

	R, Å 1.60	1.90	2.04[a]	2.30	2.70	3.10
ΔE	−3.0	−7.3	−7.8	−5.9	−3.9	−2.5
E_{ES}	−42.7	−19.0	−12.7	−7.3	−3.5	−2.0
E_{EX}	72.5	24.0	12.0	5.1	1.0	0.2
E_{PL}	−23.3	−5.0	−1.2	−1.0	−0.4	−0.1
E_{CT}	−27.1	−9.6	−5.3	−3.0	−1.2	−0.5
E_{MIX}	17.7	2.4	−0.6	0.3	0.1	0.0
$\Delta\Delta E$[b]	−25.0	−13.4	−7.3	−5.4	−2.4	−1.0
ΔES	−22.3	−10.9	−8.0	−3.1	−0.5	0.2
ΔEX	35.9	17.8	14.2	5.5	1.4	0.4
ΔPL	−48.4	−13.1	−8.4	−2.1	−0.4	−0.1
ΔCT	−51.4	−16.7	−12.3	−6.5	−3.1	−1.5
ΔMIX	60.0	9.5	5.6	0.9	0.1	0.1

[a] Energy minimum obtained from a parabolic fit. [b] Difference of energy terms between the CO-BH_3 complex (this table) and the OC-BH_3 complex (Table I). The values of Table I are fitted to rational fractions to obtain values at various R. [c] Values given in kilocalories per mole.

Table IX. Energy Decomposition Analysis for the Complex CO-BH_3, where O Is on the C_{3v} Axis and CO Is Perpendicular to the C_{3v} Axis, at Various Separations $R = r(O\cdots B)$[a]

	R, Å 2.30	2.70	3.10
ΔE	1.7	−0.1	−0.3
ES	−2.8	−0.1	0.3
EX	10.4	2.3	0.5
PL + MIX	−0.6	−0.1	−0.0
CT	−5.2	−2.3	−1.1

[a] Values given in kilocalories per mole.

Next we examine two approaches of the O end of CO to BH_3. Since CO is slightly polar with the polarity C^+O^-,[32] the approach of BH_3 to the O end may be more favorable. Table VIII lists the results of calculations for the collinear approach of O to the B end of pyramidal BH_3 maintaining C_{3v} symmetry (Figure 1E). The CO-BH_3 complex is found to be most stable at an intermolecular separation of around 2.04 Å with ΔE = −8 kcal/mol. Since the energy difference between a pyramidal and planar BH_3 (17 kcal/mol) must be added (see section IIIA), the CO-BH_3 complex is not bound with respect to the monomers. In order to facilitate a comparison between the OC-BH_3 complex and the CO-BH_3 complex, the differences of interaction energy components between the former (Table I) and the latter (Table VIII) at the same separations R are also shown in Table VIII. It is clear from these results that the instability of the OC-BH_3 complex relative to CO-BH_3 is principally due to a decrease in the charge transfer stabilization supplemented by a decrease in the electrostatic and polarization stabilization. There is a decrease in the exchange repulsion, which, in part, compensates for the other effects. The smaller CT stabilization may be attributed to two factors: that the highest occupied σ orbital of CO has a much larger distribution on C (MO coefficients for 1s, 2s, 2s′, 2pσ, and 2pσ′ orbitals are −0.14, 0.20, 0.71, −0.42, and −0.13, respectively) than on O (likewise, 0.01, −0.04, −0.07, 0.27, and 0.19), so that the CT interaction on the O side is less favored; the atomic orbitals on O are smaller than those on C, so that at an identical separation the O-B pair would have less overlap than C-B. The smaller ES may be attributed to the fact, as discussed in section IIIE, that O has a substantial positive net σ charge and a small negative net π charge, while C has the opposite charges. Apparently the σ charge controls the ES stability. The smaller EX repulsion is presumably a result of the smaller overlap mentioned above.

The second approach of O studied here is along the C_{3v} axis, while keeping CO perpendicular (staggered) to the C_{3v} axis (Figure 1F). Results in Table IX can be compared with Table VIII corresponding to Figure 1E and Table VII corresponding to Figure 1D. This perpendicular approach is less stable than the collinear approach of Table VIII mainly because of less ES stabilization and more EX repulsion, with more CT stabilization partially compensating the difference. Both perpendicular approaches which we considered were found to be repulsive. Of the two, this approach (O on the C_{3v} axis) is less repulsive than that of Table VII (C on the C_{3v} axis) due to a more favored electrostatic interaction.

IV. Borazane (H_3N-BH_3) and Derivatives: CH_3H_2N-BH_3, $(CH_3)_3N$-BH_3, and H_3N-BF_3

A. Distance Dependency. In borazane, NH_3 and BH_3 are experimentally known to be pyramidal, staggered, and oriented such that the complex maintains an overall C_{3v} symmetry. Therefore, we first carried out the energy decomposition between pyramidal NH_3 and BH_3 in the C_{3v} approach as functions of the B-N separation, $R = r(N\text{-}B)$. Results are shown in Table X. An energy minimum is found at $R = 1.70_5$ Å with a stabilization energy of 44.7 kcal/mol. This distance is in

Table X. Energy Decomposition Analysis for the Complex H_3N-BH_3 at Various Separations $R = r(N\cdots B)$[a]

	R, Å 1.46	1.56	1.66	1.705	1.86	2.30	2.70
ΔE	−33.8	−42.0	−44.66	−44.68	−41.6	−25.7	−15.0
ES	−160.7	−129.2	−103.0	−92.9	−64.8	−24.6	−11.9
EX	192.8	140.2	101.0	86.9	50.9	10.1	2.2
PL	−54.0	−33.3	−21.0	−17.2	−9.0	−2.3	−1.0
CT	−67.4	−45.6	−31.6	−27.1	−17.4	−7.8	−4.1
MIX	55.5	25.8	9.8	5.6	−1.2	−1.1	−0.2

[a] Values given in kilocalories per mole.

Table XI. Truncated Interaction Energy ΔE^{tr} and Equilibrium Separation R_e^{tr} for H_3N-BH_3, C_{3v} Approach

ΔE^{tr}	R_e^{tr}, Å	ΔE_e^{tr}, kcal/mol
ΔE	1.70	−44.7
ΔE-E_{ES}	2.54	−4.6
ΔE-E_{PL}	1.96	−33.5
ΔE-E_{CT}	2.01	−26.3

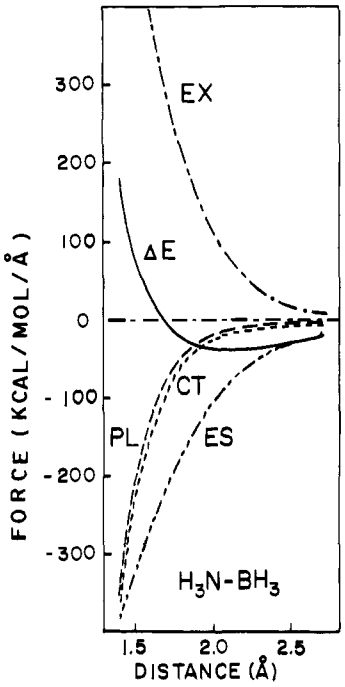

Figure 6. Force components along the separation R for the complex H_3N-BH_3 (C_{3v}, staggered) as functions of $R = r(N\cdots B)$.

reasonable agreement with the experimental value $R = 1.56$ Å.[26,33] By adding the energy (17.0 kcal/mol) required to form a bent BH_3 from a planar BH_3 the net energy of complex formation (−27.7 kcal/mol) is obtained. The experimental value for the heat of formation of this complex is not available. However, $\Delta H°_{300}$ for $(CH_3)_3N + BH_3 \rightarrow (CH_3)_3N$-$BH_3$ is −31.5 kcal/mol.[31] Since the methyl substituent effect is small both for the experimental heat of formation ($\Delta H(Me_3N$-$BH_3) - \Delta H(MeH_2N$-$BH_3) = 0.2$ kcal/mol[31]) and theoretical energy of formation ($\Delta E(Me_3N$-$BH_3) - \Delta E(H_3N$-$BH_3) = −0.6 kcal/mol, as will be discussed in section IVD), this agreement is considered to be reasonable. A more accurate comparison with the zero-point energy and correlation corrections (see section IIIA) will not be attempted here.

Near the equilibrium separation ES is the principal contributor to the stabilization, with CT and PL playing a less significant role. The relative importance of ES, CT, and PL at a larger separation (~2.70 Å) is quite similar to that near the equilibrium. We note in comparison that in OC-BH_3, all three attractions were large, of comparable magnitude, and essential contributions to the bonding. Table XI shows the equilibrium separation R_e^{tr} and the stabilization energy ΔE_e^{tr} at R_e^{tr}, which are obtained when a truncated interaction ΔE^{tr} (the total interaction energy ΔE minus a component) is used as the potential function. The lack of ES would make the complex unstable to dissociation, but the absence of PL or CT would still retain the complex's strong binding. This is in remarkable contrast with the OC-BH_3 complex, where the absence of any attractive component would make the complex unstable (Table II).

Table XII. Change of Components of Gross Atomic Population in the Complex H_3N-BH_3, C_{3v} Approach[a]

	EX	PL	CT + MIX	Total
		R = 2.70 Å		
H	0.000	−0.020	−0.007	−0.027
N	−0.000	0.061	−0.038	0.023
B	−0.002	−0.128	0.047	−0.083
H	0.001	0.043	0.004	0.047
BH_3[b]	0.0	0.0	0.059	0.059
		R = 1.70 Å		
H	0.003	−0.086	0.001	−0.082
N	−0.010	0.257	−0.188	0.059
B	−0.042	−0.062	0.036	−0.067
H	0.014	0.021	0.050	0.085
BH_3[b]	0.0	0.0	0.187	0.187

[a] Positive and negative values indicate an increase and a decrease, respectively, of electron population upon complex formation. [b] Sum of all the atoms of BH_3. The sums for NH_3 are negatives of the BH_3 values.

In Figure 6 the components of the force $-d\Delta E/dR$ as a function of the intermolecular separation R are shown. Near $R_e \sim 1.70$ Å, the relative importance of the attractive components is dES ~ 56, dPL ~ 20, and dCT ~ 24%, and at a larger separation $R \sim 2.70$ Å, the contributions are dES ~ 66, dPL ~ 7, and dCT ~ 26%. This means that the electrostatic force remains the principal bonding force as one moves from a large separation to the equilibrium distance. In OC-BH_3, quite contrary to this complex, both CT and ES were important binding forces at a large separation, and CT and PL became the dominant binding forces near equilibrium (Figure 2).

The decomposition analysis of electron distribution and gross atomic population was carried out for the complex at the separations of 2.70 and 1.70_5 Å. The component gross populations are shown in Table XII and the component electron density maps at 2.70 and 1.70_5 Å are shown in Figures 7 and 8, respectively. The population analysis at 2.70 Å and the comparison with Table II indicate that the electron population on B decreases in the order OC-BH_3 > BH_3 (pyramidal) > H_3N-BH_3. The increase in OC-BH_3 over the isolated BH_3 is due principally to CT + MIX, while in H_3N-BH_3 a similar increase is overshadowed by a large decrease resulting from PL (which is due to the larger polarity of NH_3 than that of CO). The increase in the electron population on H in BH_3 of H_3N-BH_3 over that in the isolated pyramidal BH_3 is also accountable as a PL effect. The comparable absolute magnitude of CT interaction between OC-BH_3 and H_3N-BH_3 at this distance can be seen in the CT stabilization energy (−4.3 kcal/mol for OC-BH_3 in Table I and −4.1 kcal/mol for H_3N-BH_3 in Table X) as well as in the CT component density maps in Figures 3 and 7. The increased importance of polarization in going from OC-BH_3 to H_3N-BH_3 is not obvious in the PL stabilization energy, which is small in magnitude, but is clear when the PL component density maps in Figures 2 and 7 are compared. As usual,[7] the PL map shows a sequential bond polarization $H-\delta+\delta B\cdots-\delta+\delta N-\delta+\delta H$.

Near the equilibrium geometry the reorganization picture of the electron distributions is not as simple as at a large intramolecular separation because the interaction is so strong. Nevertheless, several interesting features can be recognized in Figure 8 and Table XII. The EX effect is local as usual,[8] resulting in a small population change of the type $H-\delta B+\delta\cdot\cdot\cdot+\delta N-\delta H$. The CT picture in Figure 8 is quite different from that for OC-BH_3 in Figure 3. The CT interaction in H_3N-BH_3 near the equilibrium separation is not as strong as in OC-BH_3, as can be seen in Tables I and X. This is clearly re-

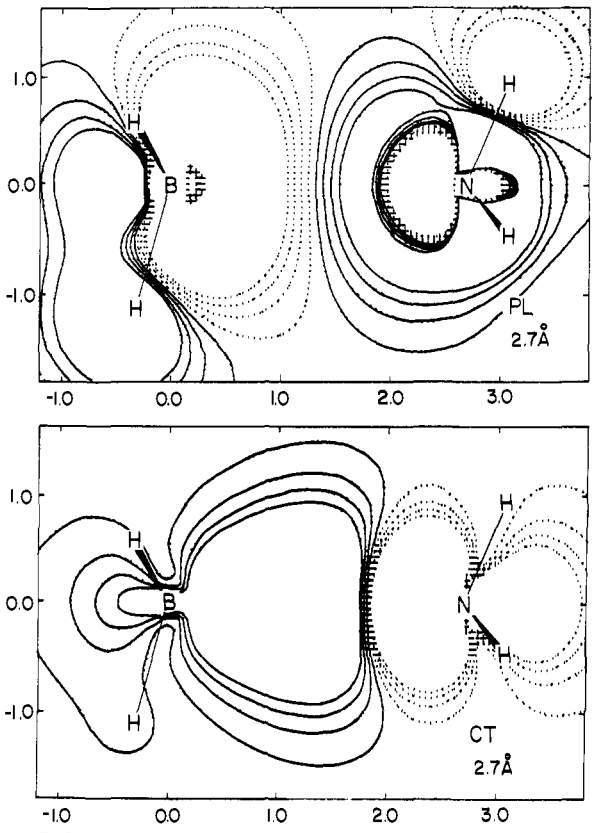

Figure 7. Component electron density maps for the complex H_3N-BH_3 at r(N···B) = 2.70 Å in the C_{3v} staggered approach. The plot is for an HBNH plane. For other details, see Figure 3.

flected in the less complete buildup of CT charge in the intermolecular region in Figure 8 than in Figure 4. The PL effect is more complicated. There is a strong polarization of NH_3 which enhances the polarity $-\delta+\delta N-\delta+\delta H$ already existing in the monomer. The polarization of BH_3 at this distance is smaller in magnitude than at a larger distance (2.70 Å), as is seen in Table XII. Furthermore, the direction of BH_3 polarization $H+\delta-\delta B$ in OC-BH_3 is opposite to that found in this complex, as may be seen by comparison between Tables III and XII and Figures 4 and 8. The difference in direction is due to the polarity difference between NH_3 (with polarity $N-\delta+\delta H$) and CO (with σ polarity $C-\delta+\delta O$ and π polarity $C+\delta-\delta O$).

An interesting question is the significance of the back-donation from BH_3 to NH_3 to total CT stabilization. Calculations at the equilibrium R = 1.70$_5$ Å give CT = −27.1, $CT_{H_3N\rightarrow BH_3}$ = −19.4, $CT_{H_3N\leftarrow BH_3}$ = −7.4, and CT_{MIX} = −0.3 kcal/mol. Although the relative contributions of these terms may sensitively depend on the basis set used, it is safe to conclude that there is a substantial contribution of the $BH_3\rightarrow NH_3$ back-donation to the stabilization. The ratio between the back and forward donation contributions $CT_{H_3N\leftarrow BH_3}/CT_{H_3N\rightarrow BH_3} \sim 1/2.6$ is not as large as the same ratio in the OC-BH_3 complex, $CT_{OC\leftarrow BH_3}/CT_{OC\rightarrow BH_3} \sim 1/2$. Furthermore, the relative importance of CT energy to the stabilization of the complex H_3N-BH_3 is rather small, and therefore, the significance of the back-donation in this complex is much less than it is in the OC-BH_3 complex.

B. Rotational Barrier. In the energy decomposition analysis we compare the energy of the complex with that of the pyramidal NH_3 and pyramidal BH_3 in the same configuration as in the complex. If one assumes that the configurations of NH_3 and BH_3 and the equilibrium r(B···N) are the same in the eclipsed conformation as those in a staggered conformation, the difference in the stabilization energy, ΔE, between the staggered and eclipsed conformations is nothing but the barrier to internal rotation, and hence the differences of energy components should be the contributions of components to the barrier. The results of such calculations at r(B···N) = 1.70$_5$

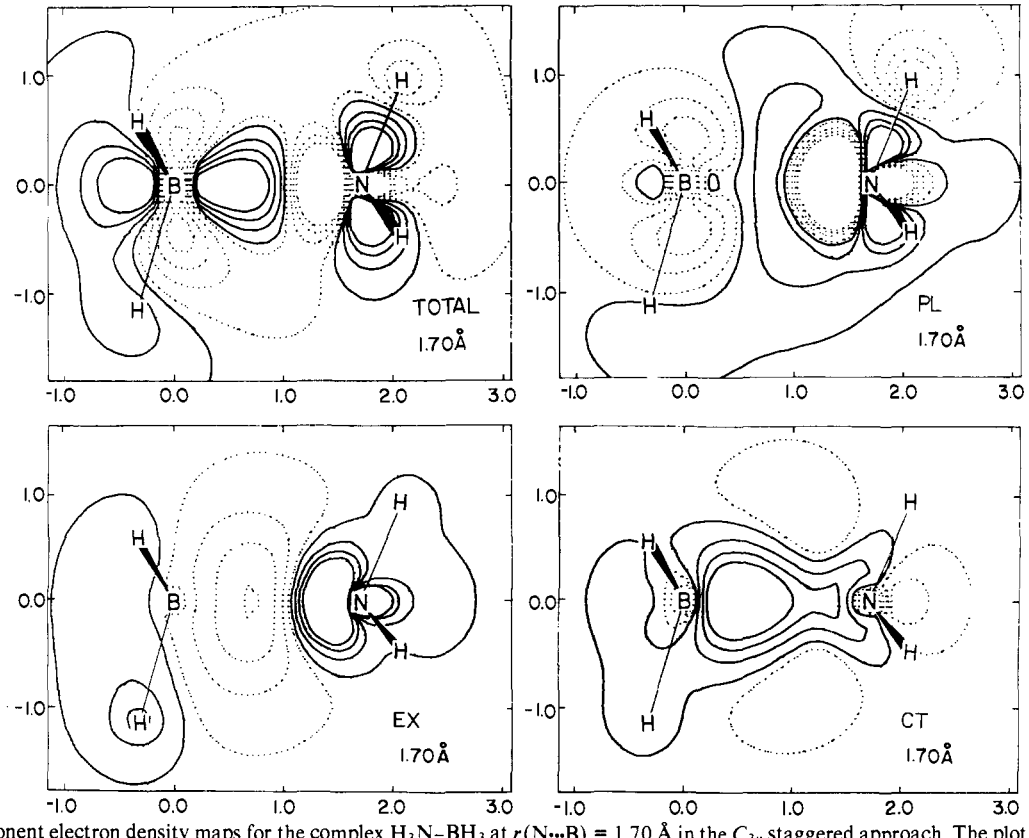

Figure 8. Component electron density maps for the complex H_3N-BH_3 at r(N···B) = 1.70 Å in the C_{3v} staggered approach. The plot is for an HBNH plane. For other details, see Figure 4.

Table XIII. Energy Decomposition of Rotational Barrier of H_3N-BH_3[a] at r(N···B) = 1.70$_5$ Å

	Staggered	Eclipsed	Difference
ΔE	−44.7	−43.2	1.5
ES	−92.9	−93.2	−0.3
EX	86.9	88.5	1.6
(overlap)	(187.2)	(190.1)	(2.9)
$(-\sum K)$	(−100.3)	(−101.6)	(−1.3)
PL	−17.2	−17.3	−0.1
CT	−27.1	−26.5	0.6
MIX	5.6	5.3	−0.3

[a] Values given in kilocalories per mole.

Å are shown in Table XIII. No experimental value for the rotational barrier of borazane is available, but calculated values, including geometry optimization, generally fall between 1.9 and 3.1 kcal/mol.[20-22,34]

From Table XIII it is clear that *the barrier is essentially caused by the difference in exchange repulsion*, while a smaller contribution to the barrier by CT is largely cancelled out by the contributions of ES, PL, and MIX. In the energy decomposition scheme of Kitaura and Morokuma the exchange energy EX can be further decomposed into two terms by the use of appropriate model Hartree-Fock operators.[8] One is a negative (attractive) contribution $(-\Sigma_i^{A\text{occ}}\Sigma_j^{B\text{occ}}K_{ij}^{0})$ of exchange integrals (called X = ESX − ES in ref 8) and the other is the positive (repulsive) contribution from the overlap integrals (called EX′ in ref 8). Table XIII shows these two exchange terms separately. The exchange integral contribution favors the eclipsed form, since B-H and N-H bonds are closer to one another in the eclipsed form, resulting in a greater attraction. This proximity of B-H and N-H bonds in the eclipsed form gives rise to a large overlap repulsion, however, which overcomes the above-mentioned attraction. Therefore, we conclude that the requirement that B-H and N-H electron distributions must be distorted and orthogonalized to satisfy the Pauli principle causes the rotational barrier.

The importance of the exchange interaction to the rotational barrier has been pointed out for ethane and methanol by Sovers, Kern, Pitzer, and Karplus in terms of bond orbitals.[35] Christiansen and Palke[36] by the use of localized orbitals and Levy et al.[37] by the use of bond orbitals recently have shown that the orbital orthogonality is the predominant factor for the barrier of ethane. We feel that an energy decomposition method, based on model Hartree-Fock operations, has advantages over other methods in that it does not require bond orbitals or localized orbitals to obtain the exchange contribution and that contributions of other energy components (ES, CT, and PL) are obtained as well on the same footing as EX. An application of the energy decomposition analysis to the barrier for internal rotation in various compounds including ethane will be presented elsewhere.[38]

C. Angular Dependency near Equilibrium Separation. In order to examine the reason why this complex prefers a C_{3v} symmetry, we tilted one or both of BH_3 and NH_3 from the C_{3v} position at the equilibrium separation r(N···B) = 1.70$_5$ Å in the staggered form. The local C_{3v} symmetry for BH_3 and NH_3 was maintained during the tilt. The tilt angles, α and β, of NH_3 and BH_3, respectively, are defined in Figure 9, where the positive directions shown by the arrows move one proton (in the plane of the paper) toward the interaction region and the other two protons away from it. Results of calculations are shown in Table XIV. The tilt $\alpha = 0 \rightarrow \alpha \neq 0$ destabilizes the complex due mainly to a reduction of the ES stabilization. Presumably this is a result of the N lone pair electrons no longer being directed toward the positively charged **B** atom. This effect occurs regardless of the sign of α and the magnitude

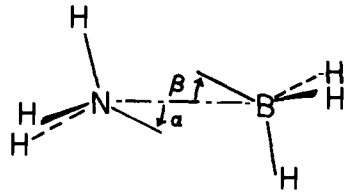

Figure 9. Tilts, α and β, of the C_{3v} axes of NH_3 and BH_3, respectively, from the N-B axis. The arrows define the positive directions of tilts.

Table XIV. Relative Energy Decomposition Analysis for the Complex H_3N-BH_3 at r(N···B) = 1.70$_5$ Å for Various Tilts of End Groups[b]

α[a] β	0° 10°	0° −10°	10° 0°	10° 10°	−10° −10°	10° −10°
$\Delta\Delta E$	2.4	2.3	1.4	5.0	4.7	2.6
ΔES	−1.3	−1.2	1.6	1.4	1.5	−0.6
ΔEX	5.0	4.5	−0.0	5.5	4.9	4.1
ΔPL	−2.2	−2.1	−0.9	−2.3	−2.3	−3.8
ΔCT	−1.7	−1.6	−0.1	−2.1	−2.0	−1.4
ΔMIX	2.7	2.6	0.8	2.5	2.6	4.4

[a] α and β are tilt angles of H_3N and BH_3, respectively, from the C_{3v} staggered symmetry, as defined in Figure 9. [b] The energy in kilocalories per mole relative to $(\alpha, \beta) = (0, 0)$.

of β. The only exception is when α and β are both nonzero and are of opposite sign. This results in a very small change in the total energy change due to cancellation of PL and MIX. The tilt $\beta = 0 \rightarrow \beta \neq 0$ destabilizes the complex rather substantially due to an increase in the EX repulsion complemented by changes in all other components. This is presumably a result of increased overlap between the N lone pair and the B-H electrons.

D. Methyl Substituent Effect. We have recently attributed a large methyl substituent effect of the proton affinity of NH_3 principally to the difference in polarization energy, though the proton affinity itself is found to be predominantly electrostatic and charge transfer in nature.[10] In connection with this it is interesting to note that the observed *N*-methyl substituent effect on the interaction energy of NH_3-BH_3 is very small ($\Delta H°_{273}$ = −17.5 kcal/mol for CH_3H_2N-BH_3, −18.9 kcal/mol for $(CH_3)_2HN$-BH_3, and −17.3 kcal/mol for $(CH_3)_3N$-BH_3 in the gas phase).[31] Table XV shows the results of calculations of *N*-methyl substituent effects for the H_3N-BH_3 complex at r(N···B) = 1.70$_5$ Å. The table also lists similar results for the proton affinity of NH_3, taken from ref 10. The calculated methyl substituent effect for the H_3N-BH_3 is very small (~1 kcal/mol), in good agreement with experiment. Successive methylation of NH_3 increases the polarization stabilization, i.e., stabilizes the complex by supplying electrons upon the approach of BH_3. The electrostatic stabilization decreases as the number of methyl groups increases, consistent with the decrease in electron density on the N atom. The charge transfer stabilization increases with methyl substitution. These trends are very similar to the proton affinity case, although the actual magnitude is smaller here because BH_3 has only a fractional net positive charge whereas H^+ has a unit charge. However, an increase in the exchange repulsion almost completely cancels out the above mentioned changes, giving rise to a very small overall methyl substituent effect. The increase in exchange repulsion obviously comes from the interaction between CH_3 groups and B-H bonds. In the case of proton affinities, the attacking H^+ does not have electrons and, therefore, there is no exchange repulsion, which leaves the polarization effect without cancellation, resulting in a large overall substituent effect.

E. H_3N-BF_3. BF_3 is usually considered to be a stronger acid,

Table XV. Energy Decomposition Analysis for Amine Methyl Substitution Effects for the H_3N-BH_3 Complex and the Protonated Complex H_3N-H^+[a]

r(N···B) = 1.705 Å	H_3N-BH_3[b]	CH_3H_2N-BH_3[c]	$(CH_3)_3N$-BH_3[c]
ΔE	−44.7	−0.8	−0.6
ES	−92.9	−1.2	0.1
EX	86.9	4.4	8.5
PL	−17.2	−5.0	−15.1
CT	−27.1	−1.4	−3.3
MIX	5.6	2.4	9.2
r(N···H^+) = 1.02 Å	H_3N-H^+[b]	CH_3H_2N-H^+[c]	$(CH_3)_3N$-H^+[c]
ΔE	−221.9	−8.5	−17.8
ES	−99.8	3.3	14.9
PL	−27.4	−12.8	−38.0
CT	−88.3	−3.4	−10.3
MIX	−6.5	4.4	15.6

[a] Proton affinity results taken from ref 10. EX = 0. Values given in kilocalories per mole. [b] Components of stabilization energy for this complex. To compare with experiment for H_3N-BH_3, the energy difference + 17.0 kcal/mol between a pyramidal BH_3 and a stable planar BH_3 has to be added to ΔE. [c] Difference between this complex and H_3N-BH_3 or H_3N-H^+.

Table XVI. Energy Decomposition Analysis for the Complex H_3N-BF_3 (C_{3v} Staggered) and Changes from H_3N-BH_3 at Various Separation $R = r$(N···B)[c]

R, Å	1.60	2.70
ΔE[a]	−71.5	−26.0
ES	−142.3	−20.5
EX	136.3	2.6
PL	−42.7	−1.5
CT	−52.7	−6.1
MIX	29.9	−0.4
$\Delta\Delta E$[b]	−28.1	−11.0
ΔES	−24.2	−8.6
ΔEX	12.9	0.4
ΔPL	−14.6	−0.6
ΔCT	−13.3	−2.0
ΔMIX	11.3	−0.2

[a] The bending energy ΔE_b = 33.0 kcal/mol required to form pyramidal BF_3 from the stable, planar BF_3 has to be added to obtain the energy of complex formation. [b] $\Delta\Delta E = \Delta E(H_3N\text{-}BF_3) - \Delta E(H_3N\text{-}BH_3)$. Same for components. The difference in the bending energy, $\Delta\Delta E_b$ = 33.0 − 17.0 kcal/mol has to be added for a comparison of the energy of complex formation. Values given in kilocalories per mole.

and hence a stronger electron acceptor in EDA complex formation, than BH_3. In order to compare contributions of energy components between the two complexes, calculations for the H_3N-BF_3 complex were performed for the staggered C_{3v} approach of NH_3 and pyramidal BF_3 at the intermolecular separations $R = r$(N···B) = 2.70 and 1.60 Å. The results are shown in Table XVI. Since it requires 33.0 kcal/mol to prepare a pyramidal BF_3 from a planar BF_3, the net ΔE for the complex formation at 1.60 Å (a near equilibrium geometry) is about −39 kcal/mol. Archibald, Armstrong, and Perkins obtained ΔE = −34.8 kcal/mol and $-\Delta H_{calcd}$ = 42 kcal/mol, which is about 13 kcal/mol greater than an experimental estimate $-\Delta H$ = 31 kcal/mol.[20b] The greater stability of the H_3N-BF_3 is principally the effect of increased ES, with PL and CT being smaller contributions. The above effects are partially negated by EX, MIX, and the difference in the deformation energy of the monomers. The increased role of ES in the H_3N-BF_3 complex may be attributed to the fact that BF_3 is more polar than BH_3. The same polarity also increases CT by making the lowest vacant BF_3 σ orbital lower in energy (0.021 Hartree vs. 0.070 in BH_3). The increase in both the PL stabilization and the EX repulsion may be attributed to the large number of electrons in BF_3 than in BH_3.

V. Conclusions and Discussions

The conclusions obtained for the OC-BH_3 complex are summarized as follows:

(i) This is a strong complex with all three attractions, ES, PL, and CT contributing significantly and almost equally to the stabilization. Lack of any one of them would make the complex unstable.

(ii) A significant relative contribution of CT even at a large intermolecular separation is unique to this complex.

(iii) Near the equilibrium geometry the contribution of the OC ← BH_3 back CT stabilization is very significant. ($CT_{OC\rightarrow BH_3}/CT_{OC\leftarrow BH_3} \sim 2/1$).

(iv) The noncollinear approach of CO is less favored than the collinear (C_{3v}) approach principally due to a decrease in ES stabilization.

(v) Pyramidal BH_3 is the favored conformation in the complex predominantly because of an increase in EX repulsion.

(vi) The approach of the O end of CO is less favored than that of the C end mainly due to a decrease in CT stabilization.

The conclusions obtained for the H_3N-BH_3 complex and its derivatives are summarized as follows:

(i) The strong binding in the H_3N-BH_3 complex is principally due to ES. The lack of ES would make the complex unstable to dissociation; however, the absence of PL or CT would still retain the complex's strong binding.

(ii) There is a substantial contribution of the $H_3N\leftarrow BH_3$ back CT stabilization (~−7 kcal/mol), but its significance to the total stabilization is not critical.

(iii) The barrier to the internal rotation of H_3N-BH_3 is essentially due to the difference in EX between the two conformers. Of the two terms in EX, the overlap repulsion term, not the exchange integral term, is responsible for the barrier.

(iv) A tilt of the C_{3v} axes of NH_3 and BH_3 from the N-B axis destabilizes the complex by reducing ES stabilization and increasing EX repulsion, respectively.

(v) The *N*-methyl substituent effect on the stability of H_3N-BH_3 is small, due to a cancellation between an increase in EX repulsion and an increase in PL stabilization. This is in contrast to the proton affinity case, where a large methyl substituent effect is due to an increase in PL stabilization.

Table XVII. Procedures of Energy Decomposition Analysis

Program	Iterations/ matrix elements included	With differential overlap	Without differential overlap	Terms obtained
Regular SCF program[a]	1st cycle[b]	ES + EX	ES	⇒ ES, EX
	SCF[b]	ΔE = ES + PL + CT + MIX	ES + PL	⇒ ΔE PL, CT + MIX
Special program[c]	Diagonal[d]	ESX = ES + X	ES	⇒ ES, X[e]
	Diagonal + $A_{occ} \rightarrow A_{vac}$[d], $B_{occ} \rightarrow B_{vac}$		ES + PL	⇒ PL
	$A_{occ} \leftrightarrow B_{occ}$[d], $A_{vac} \leftrightarrow B_{vac}$	ESX + EX′		⇒ EX′[e]
	$A_{occ} \rightarrow B_{vac}$[d], $B_{occ} \rightarrow A_{vac}$	ESX + CT		⇒ CT
	Total[d]	ΔE = ES + PL + CT + MIX		⇒ ΔE, MIX

[a] Method of Morokuma.[5-7,9] [b] The number of iterations. [c] Method of Kitaura and Morokuma.[8] [d] The matrix elements included. [e] EX = X + EX′.

(There is no cancellation because the proton has no electrons and, therefore, no EX.)

(vi) The H_3N-BF_3 complex is stronger than the H_3N-BH_3 complex, principally due to an increase in ES stabilization.

Binding of these strong EDA complexes can be compared with that of weak EDA complexes we have analyzed, including $(NC)_2CO\cdots OR_2$, $(NC)_2C{=}C(CN)_2\cdots OR_2$,[15] $(NC)_2CO\cdots C_6H_6$,[16] $H_3N\cdots F_2$, $H_3N\cdots ClF$, and $R_2CO\cdots F_2$.[39] In weak complexes, the attraction (ES + PL + CT) at a large separation (~3 Å) is relatively small, so that the exchange repulsion balances out with the attraction, preventing the donor and the acceptor from approaching closer. In strong complexes, there is a particular orientation of the donor and the acceptor, which gives rise to a large attraction and a small exchange repulsion and allows the molecules to approach closer and bind more strongly. The origin of the strong attraction at a large separation should usually be electrostatic or electrostatic plus another term or terms, since ES is the longest range interaction. For the amine-borane complexes it is essentially ES and for the OC-BH_3 complex it is ES and CT. The importance of CT at a large intermolecular separation is a unique feature that makes the complex of the relatively less polar CO very strong.

In the present paper the effects of basis functions are not examined. A recent systematic comparison of various basis sets for hydrogen-bonded complexes indicates that an addition of polarization functions (p orbitals on the hydrogen atom and d orbitals on the first row atoms) to the present 4-31G basis set corrects the overestimate of ES by reducing the polarity of individual monomers. It is found, however, that the other components are hardly affected by polarization orbitals.[38] These results lend support to the semiquantitative significance of the energy decomposition analysis described in the present paper.

Acknowledgment. The authors are grateful to Dr. S. Yamabe for helpful discussions and J. O. Noell for critical reading of the manuscript. The research is supported in part by the National Science Foundation and Public Health Research Grant No. CA-14170 from the National Cancer Institute. H.U. is on leave from Kitasato University, Tokyo, Japan.

Appendix

Procedures of Energy and Charge Decomposition Analysis.[5-9,29] In the most basic form of analysis, it is assumed that each component molecule has a closed shell configuration and retains its original geometry when the complex is formed. We usually use the following procedures to calculate the energy components (Table XVII).

(1) Calculate SCF-MO's (MO^0's) for isolated molecules. The sum of energy of the isolated molecules is called E_0.

(2) At the geometry of interest, calculate AO integrals and save them on a tape.

(3) Schmidt orthogonalize MO^0's and use them as the initial guess in the standard SCF procedure. The wave function and energy in the first cycle (before diagonalization) are

$$\Psi_3, E_3 = E_0 + E_{ES} + E_{EX}$$

and the wave function and energy after the SCF is converged are

$$\Psi_4, E_4 = E_0 + \Delta E$$
$$= E_0 + E_{ES} + E_{EX} + E_{CT} + E_{PL} + E_{MIX}$$

where ES, EX, CT, PL, and MIX refer to electrostatic, exchange, charge transfer, polarization, and coupling terms, respectively, and ΔE is the total interaction energy.

(4) Drop from the AO integral tape all the one- and two-electron integrals involving a differential overlap between the component molecules.

(5) Use the new integral tape and the MO^0's as the initial guess in the standard SCF procedure. The first cycle gives

$$\Psi_1, E_1 = E_0 + E_{ES}$$

and the converged SCF gives

$$\Psi_2, E_2 = E_0 + E_{ES} + E_{PL}$$

The above procedures, which use the standard SCF procedure twice, lead to the decomposition of ΔE into E_{ES}, E_{EX}, E_{PL}, and $E_{CT} + E_{MIX}$.

(6) In order to obtain E_{CT} separately, which requires a specially written program, follow the procedure of Kitaura and Morokuma.[8] Transform the Hartree-Fock and overlap matrices from the AO basis to the MO^0 basis and keep only interaction matrix elements connecting the occupied MO's of a molecule A with the vacant MO's of the other molecule B and the vacant MO's of A with the occupied MO's of B, in addition to the diagonal blocks. Repeat the process until the SCF is reached. The first cycle gives

$$\Psi_5, E_5 = E_0 + E_{ESX}$$

and the converged SCF yields

$$\Psi_6, E_6 = E_0 + E_{ESX} + E_{CT}$$

where ESX refers to the electrostatic plus a portion (exchange integral part) of the exchange term.[8] E_{CT} is obtained as the difference between E_6 and E_5.

(7) For the electron distribution decomposition analysis, use the method of Yamabe and Morokuma.[7] From the wave functions $\{\Psi_i, i = 1, 2, \cdots, 6\}$ obtained above, construct the one-electron density matrices $\{\rho_i\}$, which can be decomposed into individual contributions.

$$\rho_2 = \rho_1 + \rho_{PL}$$

$$\rho_3 = \rho_1 + \rho_{EX}$$

$$\rho_4 = \rho_1 + \Delta\rho = \rho_1 + \rho_{EX} + \rho_{CT} + \rho_{PL} + \rho_{MIX}$$

$$\rho_5 = \rho_1$$

$$\rho_6 = \rho_1 + \rho_{CT}$$

Here ρ_1 is the unperturbed density matrix. One way of presenting a component density matrix is a contour map as a function of the coordinates on a particular plane in space. Another is the component gross population on AO r, such that

$$N_r{}^j = (\rho_j{}^{AO}\cdot\mathbf{S}_j{}^{AO})_{rr}$$

where j = EX, CT, PL, and MIX and the superscript indicates that the matrices are in the AO basis. One may also calculate the change in the dipole moment due to each component of interaction from the corresponding component of ρ.

(8) To obtain identical results, steps 3 and 4 can also be carried out by using the special program of Kitaura-Morokuma,[8] as can be seen in Table XVII.

(9) If one wants CT to be further separated into $CT_{A\rightarrow B}$, $CT_{B\rightarrow A}$, and CT_{MIX}, carry out calculations including only the diagonal $+(A_{occ} \rightarrow B_{vac})$ blocks in the special program to obtain $CT_{A\rightarrow B}$. Diagonal $+(B_{occ} \rightarrow A_{vac})$ gives $CT_{B\rightarrow A}$. The difference between CT and $CT_{A\rightarrow B} + CT_{B\rightarrow A}$ is CT_{MIX}. Similarly PL can be separated into PL_A, PL_B, and PL_{MIX}.

(10) The method can be extended with appropriate care to open shell-closed shell and open shell-open shell interactions.[6,39]

References and Notes

(1) (a). G. Briegleb, "Electronen Donor-Acceptor Komplexes", Springer Verlag, Berlin, 1961; (b) L. J. Andrews and R. M. Keefer, "Molecular Complexes in Organic Chemistry", Holden-Day, San Francisco, Calif., 1964; (c) J. Rose, "Molecular Complexes", Pergamon Press, Oxford, 1967; (d) R. Foster, "Organic Charge Transfer Complexes", Academic Press, New York, N.Y., 1969; (e) J. Yarwood, "Spectroscopy and Structure of Molecular Complexes", Plenum Press, London, 1973.
(2) R. S. Mulliken, *J. Am. Chem. Soc.*, **72**, 600 (1950).
(3) M. W. Hanna, *J. Am. Chem. Soc.*, **90**, 285 (1968); J. L. Lippert, M. W. Hanna, and P. J. Trotter, *ibid.*, **91**, 4035 (1969). See also R. J. W. Le Fèvre, D. V. Radford, and P. J. Stiles, *J. Chem. Soc. B*, 1297 (1968).
(4) R. S. Mulliken and N. B. Person, *J. Am. Chem. Soc.*, **91**, 3409 (1969).
(5) K. Morokuma, *J. Chem. Phys.*, **55**, 1236 (1971).
(6) S. Iwata and K. Morokuma, *J. Am. Chem. Soc.*, **95**, 7563 (1973); **97**, 966 (1975).
(7) S. Yamabe and K. Morokuma, *J. Am. Chem. Soc.*, **97**, 4458 (1975).
(8) K. Kitaura and K. Morokuma, *Int. J. Quantum Chem.*, **10**, 325 (1976).
(9) K. Morokuma, S. Iwata, and W. A. Lathan in "The World of Quantum Chemistry", R. Daudel and B. Pullman, Ed., D. Reidel Publishing Co., Dordrecht, Holland, 1974, p 277.
(10) H. Umeyama and K. Morokuma, *J. Am. Chem. Soc.*, **98**, 4400 (1976).
(11) M. Dreyfus and A. Pullman, *Theor. Chim. Acta*, **19**, 20 (1970); P. A. Kollman and L. C. Allen, *J. Am. Chem. Soc.*, **92**, 753 (1970).
(12) K. Morokuma and L. Pedersen, *J. Chem. Phys.*, **48**, 3275 (1968).
(13) Recent reviews (a) P. A. Kollman and L. C. Allen, *Chem. Rev.*, **72**, 283 (1972); (b) M. D. Joesten and L. J. Schaad, "Hydrogen Bonding", Marcel Dekker, New York, N.Y., 1974.
(14) (a) H. Basch, *J. Chem. Phys.*, **56**, 441 (1972); (b) W. E. Palke, *ibid.*, **56**, 5308 (1972).
(15) W. A. Lathan and K. Morokuma, *J. Am. Chem. Soc.*, **97**, 3615 (1975). Paper 1 of the series.
(16) W. A. Lathan, G. R. Pack, and K. Morokuma, *J. Am. Chem. Soc.*, **97**, 6624 (1975). Paper 2 of the series.
(17) R. R. Lucchese and H. F. Schaefer, *J. Am. Chem. Soc.*, **97**, 7205 (1975).
(18) (a) H. Fujimoto, S. Kato, S. Yamabe, and K. Fukui, *J. Chem. Phys.*, **60**, 572 (1974); (b) S. Kato, H. Fujimoto, S. Yamabe, and K. Fukui, *J. Am. Chem. Soc.*, **96**, 2024 (1974).
(19) F. Cavallone and E. Clementi, *J. Chem. Phys.*, **63**, 4304 (1975).
(20) (a) D. R. Armstrong and P. G. Perkins, *J. Chem. Soc. A*, 1044 (1969); (b) A. M. Archibald, D. R. Armstrong, and P. G. Perkins, *J. Chem. Soc., Faraday Trans. 2*, **69**, 1793 (1973).
(21) A. Veillard, *Chem. Phys. Lett.*, **3**, 128 (1969).
(22) W. E. Palke, *J. Chem. Phys.*, **56**, 5308 (1972).
(23) W. J. Hehre, W. A. Lathan, R. Ditchfield, M. D. Newton, and J. A. Pople, GAUSSIAN 70, Program 236, Quantum Chemistry Program Exchange, Indiana University, 1974.
(24) R. Ditchfield, W. J. Hehre, and J. A. Pople, *J. Chem. Phys.*, **51**, 2657 (1969).
(25) G. Herzberg, "Electronic Spectra of Polyatomic Molecules", Van Nostrand Reinhold, New York, N.Y., 1966.
(26) E. Sutton, "Tables of Interatomic Distances and Configuration in Molecules and Ions", The Chemical Society, London, 1958.
(27) J. E. Wollrab and V. M. Laurie, *J. Chem. Phys.*, **51**, 1580 (1969).
(28) W. E. Palke and W. N. Lipscomb, *J. Am. Chem. Soc.*, **88**, 2384 (1966); M. Gelus and W. Kutzelnigg, *Theor. Chim. Acta*, **28**, 103 (1973).
(29) H. Umeyama, K. Kitaura, and K. Morokuma, *Chem. Phys. Lett.*, **36**, 11 (1975).
(30) R. L. Jaffe, T. F. George, and K. Morokuma, *Mol. Phys.*, **28**, 1489 (1974); H. S. Wall, "The Analytic Theory of Continued Fractions", Van Nostrand Reinhold, New York, N.Y., 1948.
(31) R. F. McCoy and S. H. Bauer, *J. Am. Chem. Soc.*, **78**, 2061 (1956).
(32) W. M. Huo, *J. Chem. Phys.*, **43**, 624 (1965).
(33) S. G. Shore and R. W. Parry, *J. Am. Chem. Soc.*, **77**, 6084 (1955); E. W. Hughes, *ibid.*, **78**, 502 (1956); E. L. Lippert and W. N. Lipscomb, *ibid.*, **78**, 503 (1956).
(34) A. Golebiewski and A. Parczewski, *Chem. Rev.*, **74**, 519 (1974); A. Veillard, "Internal Rotation in Molecules", W. J. Orville-Thomas, Ed., Wiley, New York, N.Y., 1974, p 385; P. W. Payne and L. C. Allen in "Modern Theoretical Chemistry", H. F. Schaefer, Ed., Plenum Press, New York, N.Y., in press.
(35) O. J. Sovers, C. W. Kern, R. M. Pitzer, and M. Karplus, *J. Chem. Phys.*, **49**, 2592 (1968); C. W. Kern, R. M. Pitzer and O. J. Sovers, *ibid.*, **60**, 3583 (1974).
(36) P. A. Christiansen and W. E. Palke, *Chem. Phys. Lett.*, **31**, 462 (1975).
(37) M. Levy, T. S. Nee, and R. G. Parr, *J. Chem. Phys.*, **63**, 316 (1975).
(38) H. Umeyama and K. Morokuma, unpublished work.
(39) H. Umeyama, K. Morokuma, and S. Yamabe, unpublished work.